JOURNAL OF GEOPHYSICAL RESEARCH, VOL. 106, NO. D21, PAGES 27,757-27,768, NOVEMBER 16, 2001

An extension of Measurement of Ozone and Water Vapour by Airbus In-service Aircraft (MOZAIC) ozone climatologies using trajectory statistics

Andreas Stohl, Paul James, Caroline Forster, and Nicole Spichtinger

Lehrstuhl für Bioklimatologie und Immissionsforschung, Technical University of Munich, Freising, Germany

Alain Marenco and Valérie Thouret

Laboratoire d'Aérologie, Université Paul Sabatier, Toulouse, France

Herman G. J. Smit

Forschungszentrum Jülich, Jülich, Germany

Abstract. This study investigates the distribution and the sources of ozone (O_3) observed in the uppermost troposphere and lowermost stratosphere within the framework of the Measurement of Ozone and Water Vapor by Airbus In-Service Aircraft (MOZAIC) program. The O_3 measurement data taken aboard five commercial aircraft during a 1-year period are combined with 8-day three-dimensional back trajectories ending at the aircraft positions. Potential vorticity along the trajectories is used to form subsets of the data taken in the troposphere, in the stratosphere, and in stratosphere-troposphere exchange flows. A measured O_3 value is then attributed to the entire path of the corresponding trajectory. A statistical analysis of this data set extends previous global MOZAIC O_3 climatologies which are restricted to the major flight corridors. Furthermore, it allows source region identification of the measured O_3. It is found that the North American and Eurasian continental boundary layers are the major sources of upper tropospheric O_3 in spring and summer, while the African boundary layer is the greatest O_3 source in fall and winter. The seasonal O_3 variation is strongest in air masses exported from central Asia, followed by North America. The central Asian O_3 maximum is higher and occurs earlier in the year than the North American maximum, which possibly indicates a great influence from biomass burning emissions in Asia. In the lowermost stratosphere the dominant structures in the O_3 distribution are a strong north-south gradient and a wave-like pattern with O_3 maxima over North America and eastern Asia. O_3 concentrations in stratosphere-troposphere exchange flows are higher than in tropospheric air throughout the year and thus provide an important O_3 source for the troposphere. However, our analysis suggests that photochemical O_3 formation is more important than stratosphere-troposphere exchange during most of the year.

1. Introduction

The four-dimensional climatological distribution of O_3 in the troposphere and lowermost stratosphere is known only with relatively large uncertainty. The existence of numerous surface O_3 monitoring networks has led to a relatively good knowledge of the seasonal and spatial variations of O_3 in the boundary layer, but there is still a lack of measurement data throughout the free troposphere and lowermost stratosphere. Aircraft measurement campaigns, although important in improving our knowledge of the processes controlling O_3 are inappropriate for building O_3 climatologies because they provide neither the necessary global coverage nor the seasonal information. Until recently, the only data source for establishing O_3 climatologies was the global ozonesonde network [e.g., *Logan*, 1999; *Beekmann et al.*, 1994], which has a rather poor global coverage. Satellite data, such as from the Total Ozone Mapping Spectrometer, have global coverage, but the vertical resolution, if so any, is inadequate to infer much more than tropospheric columns [e.g., *Fishman et al.*, 1990].

Paper number 2001JD000749.
0148-0227/01/2001JD000749$09.00

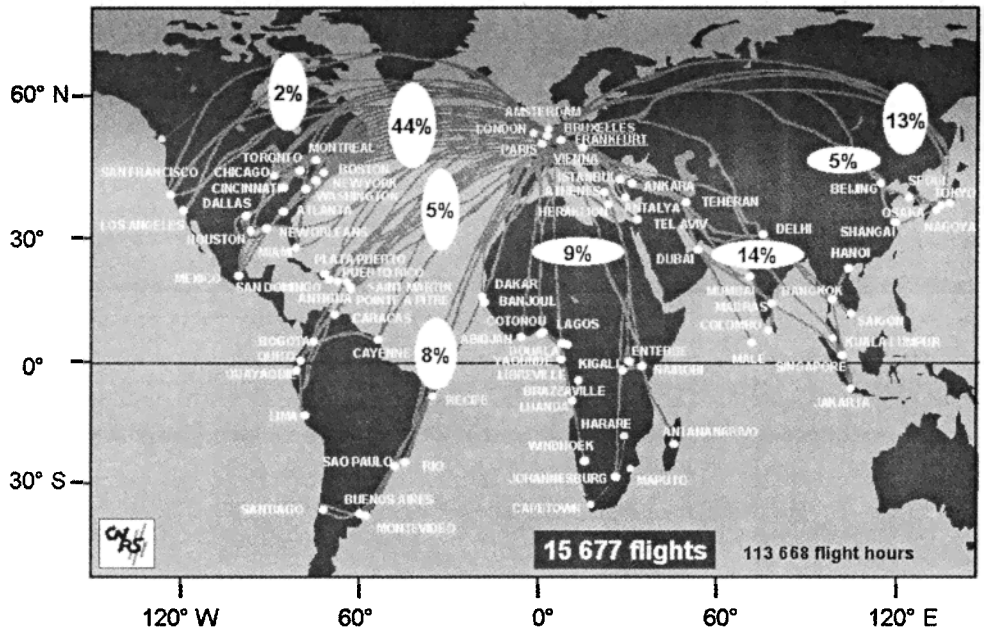

Figure 1. Geographical coverage of the MOZAIC program, with indications of the percentage of flights in the major directions (September 1994 to November 2000).

In the last few years, a few commercial airliners were equipped with O_3 sensors [*Brunner et al.*, 1998; *Marenco et al.*, 1998] which has increased available O_3 data in the free troposphere tremendously. The spatial coverage of all flights performed within Measurement of Ozone and Water Vapor by Airbus In-Service Aircraft (MOZAIC), the most comprehensive of these monitoring programs, is shown in Figure 1. The measurements are restricted to the major flight corridors and, with the exception of ascents and descents near airports, to the flight levels at 9-12 km. On the other hand, air masses are transported to the flight corridors from various regions, and because of the lifetime of O_3 of about 1 month in the free troposphere [*Liu et al.*, 1987], these air masses carry information on the O_3 concentrations in regions upwind of those actually flown through. In this paper we combine O_3 measurements from the MOZAIC program [*Marenco et al.*, 1998] with back trajectories to learn about the global distribution of O_3, thereby extending the available MOZAIC O_3 climatology presented by *Thouret et al.* [1998].

Photochemical models are presently the only tool available to distinguish between the relative contributions of different O_3 sources to the global budget. The models suggest that photochemical O_3 formation from anthropogenic precursors is the largest source in the Northern Hemisphere [e.g., *Lelieveld and Dentener*, 2000], but as the results are still poorly constrained by measurements and have considerable uncertainties, a confirmation independent from photochemical modeling is desirable. In addition to providing an O_3 climatology, this study also aims at identifying the source regions of O_3 on a global scale using only measurement data and back trajectories.

2. Measurement Data, Trajectory Model, and Analysis Method

2.1. Measurement Data

In this paper we use O_3 data collected with five commercial airliners equipped with O_3 sensors (precision better than ± 2 ppb) within the MOZAIC program [*Marenco et al.*, 1998]. MOZAIC data have been used previously by numerous authors to establish O_3 climatologies [e.g., *Thouret et al.*, 1998], to study layers in the troposphere [e.g., *Newell et al.*, 1999], and to validate chemistry transport models [e.g., *Law et al.*, 2000]. Data from about eight flights per day are available in the MOZAIC database. We used integrated data with a time resolution of at least 1 min and a vertical resolution of 150 m or better. At flight level each data point represents a flight segment of approximately 15 km. Measurements taken in the boundary layer may be influenced by local contamination, especially because the aircraft descend and ascend close to big cities. Therefore we used data from above the 700 hPa level only. The data cover the period November 1999 to October 2000 and comprises a total of some 1.4 million 1-min averages.

2.2. Trajectory Model

We calculated three-dimensional 10-day back trajectories ending at all aircraft positions where measurements were taken using the FLEXTRA trajectory model [*Stohl et al.*, 1995; *Baumann and Stohl*, 1997; *Stohl and Seibert*, 1998]. FLEXTRA is driven with global analysis fields every 6 hours and with 3-hour forecast fields every other 3 hours. The wind fields have a

resolution of 1° longitude × 1° latitude and were retrieved from the *European Centre for Medium-Range Weather Forecasts* (*ECMWF*) [1995] archives. In October 1999 the ECMWF model resolution was enhanced to 60 model levels, which is equivalent to a spacing between model levels of approximately 700 m at the typical MOZAIC aircraft cruising altitude, and much less below. As our period of study was November 1999 to October 2000, all wind fields we used have an excellent vertical resolution in both the troposphere and the stratosphere. FLEXTRA uses bicubic horizontal, quadratic vertical, and linear time interpolation. No isentropic assumption is invoked, which is important especially for ascending airstreams, where condensation causes diabatic heating. While small-scale convective cells are not resolved, the general characteristics of larger convective regions are well captured, resulting in upward transport in these regions. The vertical positions of the ending points of the back trajectories were determined by matching the pressure measured by the aircraft with the pressure of the ECMWF analyses. Trajectory positions were stored every 3 hours together with potential vorticity (PV) interpolated from the ECMWF analyses.

2.3. Data Classification

O_3 concentrations and O_3 sources vary considerably throughout the year. Therefore we carried out our analyses separately for each of the four seasons, winter (December to February), spring (March to May), summer (June to August), and fall (September to November). The seasons refer to the Northern Hemisphere, as most of the data were obtained there.

O_3 concentrations differ strongly in the troposphere, in the stratosphere, and in air masses that have recently been transferred from the troposphere to the stratosphere (troposphere-stratosphere exchange flows, TSE) or vice versa (stratosphere-troposphere exchange flows, STE). PV is a quasi-conservative tracer that is high in the stratosphere and low in the troposphere. It is modified by diabatic heating or cooling only. The PV definition of the tropopause is not applicable in the tropics, but there all data are sampled well below the tropopause and can be considered tropospheric. We therefore classified data as purely tropospheric when the PV of all trajectory positions was less than 2 PV units (1 pvu=1×10^{-6} m^2 K kg^{-1} s^{-1}) (> −2 pvu in the Southern Hemisphere); purely stratospheric when the PV of all trajectory positions was greater than 2 pvu; TSE when the PV at the measurement location was greater than 2 pvu but the minimum PV along the trajectory was less than 2 pvu; and STE when the PV at the measurement location was less than 2 pvu but the maximum PV along the trajectory was greater than 2 pvu. The first two criteria distinguish very strictly between purely tropospheric and purely stratospheric air as they require air to have been residing in the respective atmospheric compartiment for at least 10 days. STE and TSE flows, however, are difficult to distinguish, because many of the respective trajectories travel back and forth across the 2 pvu surface, possibly leading to multiple exchange events between the troposphere and the stratosphere (H. Wernli and M. Bourqui, A one-year Lagrangian "Climatology" of (deep) cross-tropopause exchange on the extratropical Northern Hemisphere, submitted to *Journal of Geophysical Research*, 2001) (hereinafter referred to as (Wernli and Bourqui, submitted manuscript, 2001)). Thus both STE and TSE air masses have stratospheric as well as tropospheric characteristics and should be viewed as transitional airflows in the tropopause region. We also present a sensitivity study using more strict definitions of STE and TSE.

A critical point in the data classification is the resolution of exchange processes between the stratosphere and troposphere in the ECMWF data. We have good experience in using PV and trajectories based on ECMWF data for this purpose, even with previously available coarser vertical resolution [*Stohl and Trickl*, 1999; *Stohl et al.*, 2000]. But sometimes stratospheric intrusions and lower tropospheric air masses can come very close together [*Parrish et al.*, 2000; *Prados et al.*, 1999]. In these cases the PV of the originally stratospheric air mass will typically have decreased to tropospheric values and, due to limited resolution, the trajectories may not trace the air mass back into the stratosphere, leading to a misclassification. To explore the possible effect of such misclassifications on our results for purely tropospheric air, we make three sensitivity studies: First, we decrease the PV threshold to 1 pvu. Second, in conjunction with the 2 pvu threshold we use the MOZAIC humidity data to exclude particularly dry air masses. Third, we use only a humidity criterion.

Mixing of stratospheric intrusions into the troposphere blurs the relations between O_3 and both humidity and PV [*Beekmann et al.*, 1994]. The originally stratospheric O_3 participates in non linear photochemical processes and eventually becomes part of the tropospheric O_3 budget. At that stage, a classification of O_3 in the troposphere as being stratospheric becomes meaningless, even though there may be still some contribution from the stratosphere. Thus our results for the troposphere still reflect some stratospheric "background" influence. Possibly, some STE events that have been misclassified as tropospheric air may have some influence as well.

2.4. Trajectory Statistics

The trajectory statistics method we use is related to flow climatologies [*Miller*, 1987], cluster analysis [*Moody and Galloway*, 1988], and residence time analysis [*Ashbaugh et al.*, 1985]. All these methods have been used to obtain qualitative information on the pathways that deliver polluted air masses to a receptor site [see *Stohl*, 1998].

Seibert et al. [1994] and *Stohl* [1996] developed more

quantitative methods that were recently tested by *Wotawa and Kröger* [1999] on their ability to reconstruct emission inventories. With each of these methods, a measured concentration is attributed to all points of its corresponding back trajectory. Thus the measured concentration is smeared out along the path the air has taken before arriving at the measurement location. After this is done for all trajectories, a so-called "concentration field" is obtained by averaging all values that occur within a grid box. This field is smoothed with the restriction that all averages are kept within their 99% confidence intervals [*Seibert et al.*, 1994]. In this study we used a global grid with a horizontal spacing of 10° longitude ×6° latitude and three vertical layers from the surface to 700 hPa, 400-700 hPa, and above 400 hPa for evaluating the concentration fields.

The concentration field can be interpreted in two ways. Assuming that the substance studied is a passive tracer, the concentration field represents its "true" average spatial concentration distribution under the condition that transport takes the air to the receptor locations, in our case, the flight tracks of the MOZAIC aircraft. If the meteorological or chemical environment under this condition differs from the average one, the concentration field may be different from an unconditioned field as it would be obtained by averaging in situ measurements throughout the region. As an example, O_3 concentrations in the lowest layer of the field may be different from the true average ones, since airflows are required to ascend to the aircraft tracks, and upward transport occurs under specific meteorological conditions. The second interpretation of the concentration field is that it shows the source (sink) regions of the substance, that is, regions from where high (low) concentrations are advected toward the receptors. This, however, requires the sources to be reachable by the back trajectories which, because of the long lifetime of stratospheric O_3, is not the case in the stratosphere. Therefore the stratospheric concentration fields should be interpreted more under the aspect of the concentration distribution in the lower stratosphere rather than as the identification of stratospheric O_3 sources. In summary, one can perceive the concentration fields either as source (sink) regions for the receptors or, with the condition that transport to the receptor must occur, as average spatial distributions. While these two aspects appear to be very different from each other, and each has its own limitations, they are intimately tied together by the transport.

The method of *Stohl* [1996], in an iteration process, could subsequently improve on this concentration field in order to reconstruct the sharp gradients typically found in the emission fields of many substances, and which are smeared out along the trajectories with the above procedure. However, Stohl's method depends critically on the condition of strictly linear chemistry and temporally constant emission fields of a substance and is thus not applicable to O_3. Thus redistribution was not applied. Even with Seiberts method, the assumption of O_3 being a passive tracer over the duration of the back trajectories is critical. If not fulfilled, it invalidates the attribution of a concentration to all points of a back trajectory. But since the lifetime of O_3 in the free troposphere is of the order of 1 month [*Liu et al.*, 1987], the error introduced by this assumption is acceptable. Furthermore, we tested the sensitivity of the concentration field to the length of the trajectories by applying the method with 2-day, 5-day, 8-day, and 10-day trajectories and found our main results to be unaffected (see section 3). We finally used 8-day trajectories, which is a compromise between a good geographical coverage of the climatology (the longer the trajectories the better the coverage) and the ability to detect smaller-scale features (using long trajectories tends to smooth the concentration patterns).

Trajectory accuracy is important, because trajectory errors lead to a smoothing of the concentration field. It is unlikely, though, that with a large data set random trajectory errors can generate spurious concentration maxima. Thus we require a minimum of 100 trajectories to pass through a grid box in order for a value to be reported. An important exception is deep convection which is not resolved by the trajectories and occurs systematically over certain regions. If O_3 from an actual boundary layer source is lifted by convection to the upper troposphere, the concentration field would show a maximum at high levels, where the trajectories pass through the convective cells. While the horizontal position of the O_3 source would still be determined correctly, its vertical position would be shifted to higher levels. This has to be kept in mind when interpreting the results, especially in the tropics.

The quality of the concentration field also depends on the density of the observations. Where the results are poorly constrained by measurements (e.g., there are no MOZAIC measurements over the Pacific, see Figure 1), the results are more uncertain than in other regions and show less details.

3. Results

3.1. Air Mass Statistics

Table 1 presents the frequency (percent) of O_3 measurements taken in purely tropospheric and in purely stratospheric air, and in STE and TSE flows, respectively, for three latitudinal belts and for the four seasons. In the tropical belt from 15°S to 21°N more than 90% of the measurements were done in the troposphere, and the rest in STE and TSE flows, while very few data were sampled in stratospheric air. In the middle latitudes (21°N to 57°N), tropospheric measurements are most frequent in summer, when the tropopause is highest, whereas stratospheric measurements are most frequent in winter, when the tropopause is lowest. Here the frequency of both STE and TSE air masses is the highest of the three latitudinal belts, consistent with

Table 1. Frequency of O_3 Measurements Above 700 hPa Taken in Purely Tropospheric, in Purely Stratospheric Air, and in STE and TSE Flows for Three Latitudinal Belts and for the Four Seasons [a]

Latitudinal Belt	Season	Tropospheric	Stratospheric	STE	TSE
15° S - 21° N	spring	92	0	4	4
15° S - 21° N	summer	93	0	4	4
15° S - 21° N	fall	93	0	4	3
15° S - 21° N	winter	90	0	6	4
21° N - 57° N	spring	31	36	14	19
21° N - 57° N	summer	39	28	13	20
21° N - 57° N	fall	34	34	14	19
21° N - 57° N	winter	27	46	11	16
57° N - 90° N	spring	14	70	6	11
57° N - 90° N	summer	14	65	7	14
57° N - 90° N	fall	11	71	7	11
57° N - 90° N	winter	12	77	4	7

[a] Units in percent.

the position of the tropopause break associated with the polar front where most of the exchange takes place. At high latitudes, most of the measurements were done in the stratosphere. At middle and high latitudes, TSE and STE airflows can be expected to have similar frequency [*Stohl*, 2001; Wernli and Bourqui, submitted manuscript, 2001], even though the net effect will be a mass transfer into the troposphere (net STE). The higher frequency of TSE airstreams in the middle and higher latitudes as seen in Table 1 is likely due to the flight routing of commercial aircraft that favors flights in the stratosphere. Furthermore, commercial aircraft avoid the turbulent regions of tropopause folds and may thus sample fewer STE events.

O_3 mixing ratios in these air masses are very different from each other (Table 2). Tropospheric O_3, with the lowest concentrations of all classes, has a clear summer peak and a winter minimum in all three latitudinal belts. The highest concentrations are observed in the middle latitudes, except in winter when they are highest in the tropics. Stratospheric O_3 has a distinct spring maximum and a fall minimum in the middle and higher latitudes.

Both STE and TSE flows have concentrations intermediate between the tropospheric and the stratospheric classes. Interestingly, STE O_3 concentrations are much lower than those in TSE flows. There are three possible explanations for the TSE O_3 concentrations being higher than the STE ones. First, many of the TSE air parcels, although temporarily residing in the troposphere, actually originate in the stratosphere. It is known that a significant branch of an airflow descending into the troposphere returns to the stratosphere shortly after a STE event [e.g., *Vaughan et al.*, 1994] and thus still contains stratospheric O_3 concentrations. Second, errors in the trajectories may suggest a STE or TSE event, while in reality the air stayed in the respective compartiment. Third, mixing brings O_3 concentrations in STE and TSE flows closer to those in the surrounding air.

To explore this in more detail, we redefined STE and TSE flows using more strict criteria: STE flows are sam-

Table 2. Average O_3 Mixing Ratios Measured Above 700 hPa in Purely Tropospheric, in Purely Stratospheric Air, and in STE and TSE Flows for Three Latitudinal Belts and for the Four Seasons [a]

Latitudinal Belt	Season	Tropospheric	Stratospheric	STE	TSE
15° S - 21° N	spring	51	-	76	117
15° S - 21° N	summer	58	-	78	105
15° S - 21° N	fall	47	-	55	80
15° S - 21° N	winter	47	-	59	88
21° N - 57° N	spring	63	340	83	168
21° N - 57° N	summer	69	268	86	140
21° N - 57° N	fall	50	173	61	93
21° N - 57° N	winter	45	244	60	104
57° N - 90° N	spring	58	428	78	194
57° N - 90° N	summer	64	335	86	163
57° N - 90° N	fall	51	222	60	107
57° N - 90° N	winter	43	311	55	121

[a] Units in ppb.

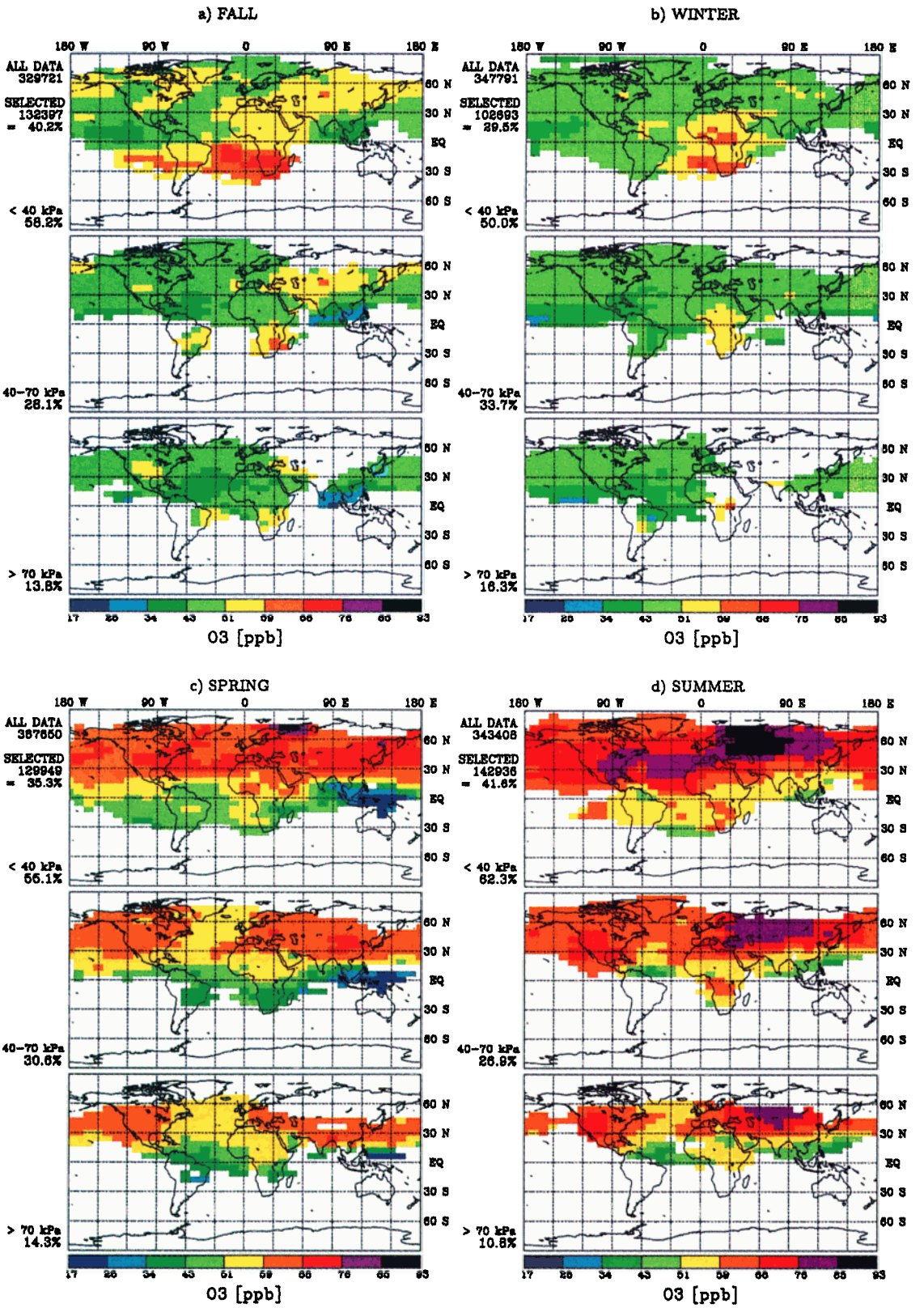

Plate 1. O_3 concentration fields obtained with trajectory statistics for purely tropospheric data for each of the four seasons: (a) fall, (b) winter, (c) spring, and (d) summer. Shown in each panel are the results for altitudes (top) above 400 hPa, (middle) between 400 and 700 hPa, and (bottom) below 700 hPa. Grid boxes containing less than 100 trajectories are left blank. On the left-hand side of each panel "ALL DATA" gives the number of all MOZAIC O_3 measurements available, and "SELECTED" indicates the number of purely tropospheric measurements that were used in this plot. The percentages given below the pressure ranges give the frequency of trajectory points falling into the respective level.

pled in air with PV<1 pvu but the maximum PV along the trajectories is greater than 3 pvu. TSE flows are sampled in air with PV>3 pvu but the minimum PV along the trajectories is less than 1 pvu. This led to a small decrease of O_3 concentrations in STE flows and a small increase of O_3 concentrations in TSE flows. This excludes multiple fluctuations around the tropopause as being the reason for the higher TSE O_3 concentrations compared to the STE ones. Thus trajectory errors or mixing must be responsible. It is not unlikely, though, that mixing is the main reason, because observations show that stratospheric intrusions into the troposphere, once below the 2 pvu threshold, are rarely ever associated with O_3 concentrations much above 100 ppb [*Stohl et al.*, 2000; *Stohl and Trickl*, 1999], which would be typical for the stratosphere. Similarly, tropospheric intrusions observed in the stratosphere have typical O_3 mixing ratios above 100 ppb [*Vaughan and Timmis*, 1998]. Thus the result that STE airflows have lower O_3 concentrations than TSE airflows does not contradict observational case studies of these airstreams.

Both the rather low frequency of STE air masses and the fact that O_3 in these air masses is enhanced only moderately over tropospheric values suggest that STE, although certainly a contributing factor, is less important than photochemical O_3 formation for the upper tropospheric O_3 budget.

3.2. Troposphere

Plate 1 shows the concentration fields for purely tropospheric O_3. In fall and winter, the highest O_3 concentrations occur in the equatorial and southern subtropical region, and particularly over Africa. The maximum over Africa is found both at the uppermost level (i.e., pressure below 400 hPa) and for air masses ascending from the 400-700 hPa level. There are relatively few air parcels ascending from the lowest (i.e., pressure greater than 700 hPa) level, but it is very likely that also the upper tropospheric maximum is the signal of photochemically produced O_3 lifted from the surface by convection. Particularly, African savanna fires peak during this season [*Cahoon et al.*, 1992] and cause significant O_3 production. Lightning, which produces NO_x, also has a maximum over the African continent [*Christian et al.*, 1999] and may contribute also to the O_3 maximum. The fact that no significant maximum is identified over South America is likely due to the poor coverage of this region by MOZAIC flights. Generally, our results are in agreement with the idea that in the tropics the ascending branch of the Walker circulation heaves polluted air masses into the upper troposphere over the continents, causing upper tropospheric O_3 maxima [*Jacob et al.*, 1996]. The small maxima over North America and Eurasia in fall are a signal of fading summer time photochemistry in September.

In spring and summer, the spatial gradients in the tropospheric O_3 concentration fields are greater than during fall and winter. The highest O_3 values are found in the Northern Hemisphere middle latitudes and the lowest ones occur in the Asian monsoonal flow. Especially in summer, there are distinct maxima over the North American and the Eurasian continents. These maxima are found at all levels, pointing toward the importance of convection, but the patterns are most pronounced for the lowest level, confirming that much of the vertical motion is resolved by the trajectories. Air masses that are lifted from the North American or Eurasian boundary layer have O_3 mixing ratios in the range of 60-80 ppb, whereas air masses lifted from the North Atlantic have O_3 mixing ratios of only about 40-55 ppb. Some of the oceanic air masses may have been ascending right from the maritime boundary layer, where O_3 concentrations are low [*Oltmans and Levy*, 1994] because of photochemical destruction. This is a very strong indication for the importance of photochemical O_3 formation in the continental boundary layers and subsequent export of O_3 pollution to higher levels for the global tropospheric O_3 budget. A case study of such an O_3 transport from the North American boundary layer to the uppermost troposphere was recently presented by *Stohl and Trickl* [1999]. Plate 1 documents that in spring and summer such events must be very frequent and are possibly the major source of O_3 in the upper troposphere. This strong impact of O_3 formed in the continental boundary layers on upper tropospheric O_3 is due to both convection over the heated landmasses and frontal uplifting downwind of the continents [*Stohl*, 2001]. Compared to this, low-level outflow of O_3 from the continental rims [*Parrish et al.*, 1993; 1998; *Crawford et al.*, 1997] may be much less important for the global O_3 budget. The fact that the continental O_3 sources are revealed so clearly by our method also makes it unlikely that O_3 formation in the background global troposphere plays an equally important role.

Perhaps surprising is that the O_3 maximum over Eurasia is higher than the one over North America. Also, its position is in poor agreement with inventories of anthropogenic O_3 precursor emissions [e.g., *Benkovitz et al.*, 1996]. Because of the coarse resolution of our method, several smaller maxima that may actually exist over Asia may be smoothed out, yielding a single maximum over central Asia. However, intense (though not exceptionally intense) biomass burning (about 1 million ha of forest burned in Siberia according to official estimates, see http://www.ruf.uni-freiburg.de/fireglobe/current/archive/archive.htm) occurred in Siberia in the year 2000. As continental-scale O_3 plumes can form from boreal forest fire emissions [*Wotawa and Trainer*, 2000; C. Forster et al., Transport of forest fire emissions from Canada to Europe, accepted by *Journal of Geophysical Research*, 2001; S. A. McKeen et al., Ozone production from Canadian wildfires during June and July of 1995, submitted to *Journal of Geophysical Research*, 2001], this may be an explanation for the location of the Asian O_3 maximum.

In order to analyze the seasonal cycle of photochem-

Table 3. Definition of the Boxes Used to Study the Seasonal Variation of Tropospheric O_3

Box Name	Longitude Range	Latitude Range
North America	120° W - 80° W	30° N - 48° N
Central Asia	40° E - 100° E	36° N - 60° N
North Atlantic	50° W - 20° W	30° N - 60° N
Southern Africa	10° E - 30° E	24° S - 0° N
Tropical Atlantic	40° W - 10° W	12° S - 12° N
Maritime continent	90° E - 150° E	12° S - 18° N

ically produced O_3 in more detail, we recalculated the trajectory statistics for each of the 12 months separately but evaluated the concentration fields for a few large regions only. These regions were defined by latitude-longitude boxes as shown in Table 3. To concentrate on cases with upward transport to the flight levels, the two lowermost layers (reaching from the surface up to 400 hPa) were combined. O_3 values associated with trajectory points falling into the respective boxes were averaged and are reported as monthly means. The selection of the boxes was done in order to contrast the strongest source regions of photochemically produced O_3 found in Plate 1 with remote ocean areas.

The results are shown in Figure 2. The most striking feature is the large seasonal cycle in all three of the Northern Hemisphere mid latitude boxes. The summertime peak indicates strong photochemical activity. The annual variation is much stronger in the continental (North America, central Asia) boxes than in the North Atlantic box, in agreement with the theory that O_3 formation in the continental boundary layers exerts the largest influence on upper tropospheric O_3. The summer maximum over the North Atlantic is likely due to outflow from the continents, which is supported by the fact that it is less strong in the lowermost layer (surface to 700 hPa). Interestingly, the central Asia box shows a higher summer time peak (83 ppb) than the North America box (71 ppb), whereas O_3 concentrations in other seasons are very similar to North America. Furthermore, the summer peak is much sharper and occurs in June, while the North America box shows a broader summer maximum peaking in August. The reason for these differences is not clear. Since the central Asia box is located further north than the North America box, photochemical processes therein may be more sensitive to the decline of solar radiation after June. Another important difference between the two boxes is that while the North America box covers a region of strong anthropogenic O_3 precursor emissions, anthropogenic emissions in the central Asia box are much lower. However, according to official reports, approximately 200,000 ha of forested and more than 100,000 ha of non forested land were burned by wildfires from June 1 to July 12, 2000. It seems plausible that this peak in fire activity contributed significantly to the maximum in O_3 production in June.

O_3 concentrations in the tropical boxes are lower than those in the northern mid latitudes during most of the year (note that the curves for southern Africa, the tropical Atlantic, and the maritime continent have been offset by -20 ppb in Figure 2 for clarity of presentation). The smallest variation is found over the tropical Atlantic, where O_3 ranges from about 40 to 50 ppb throughout the year. This reflects the absence of O_3 production and suggests O_3 import from other regions. The lowest concentrations, ranging from 24 ppb in March to 50 ppb in June are found in the maritime continent box. Higher O_3 concentrations can be expected there in El Niño years, when due to the dry conditions intense biomass burning takes place [*Thompson et al.*, 2001]. But in more normal years, like 2000, the sunlit and moist tropical maritime boundary layer is a highly efficient O_3 sink. The highest O_3 concentrations in the tropics are found in the southern Africa box. The maximum (66 ppb) occurs in austral spring and summer, likely due to both biomass burning and anthropogenic emissions. The high value for February

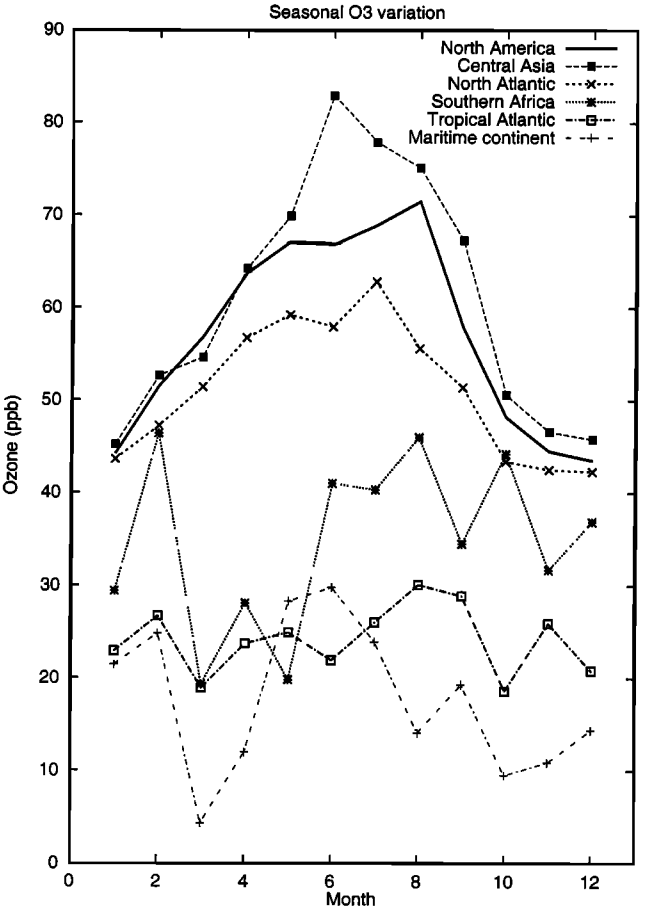

Figure 2. Seasonal variation of the O_3 mixing ratios as obtained with trajectory statistics for the six grid boxes defined in Table 3. Only data from the two lowest layers (i.e., below 400 hPa) were used. For clarity of presentation, the curves for southern Africa, equatorial atlantic and maritime continent were shifted by -20 ppb.

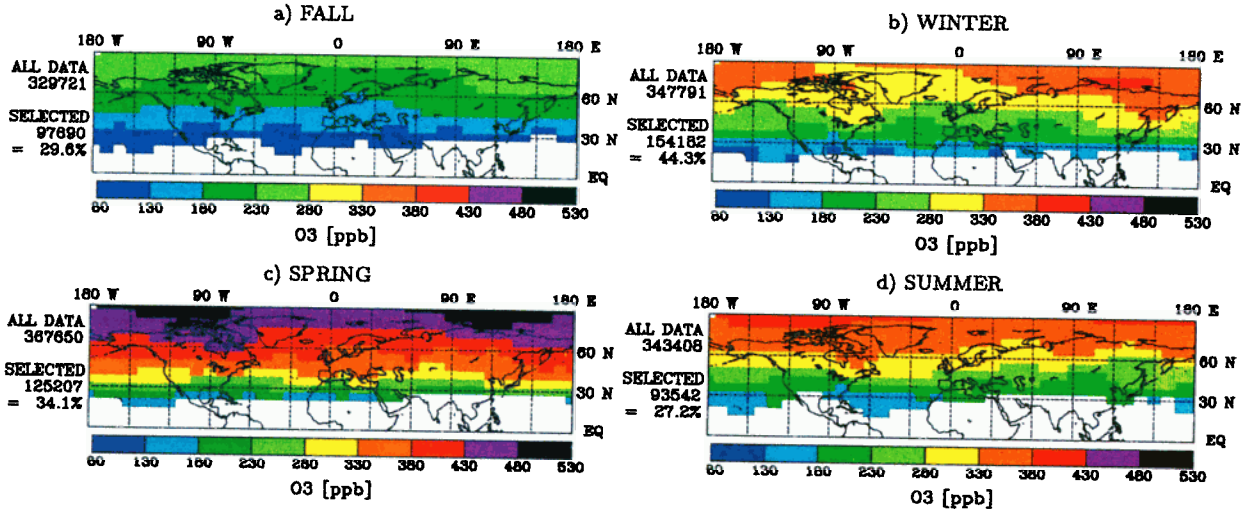

Plate 2. O_3 concentration fields summarized over all altitude levels obtained with trajectory statistics for purely stratospheric data taken during the four seasons: (a) fall, (b) winter, (c) spring, and (d) summer. On the left-hand side of each panel "ALL DATA" gives the number of all MOZAIC O_3 measurements available, and "SELECTED" indicates the number of purely stratospheric measurements that were used in this plot.

may be an artifact since the number of available trajectory points was more than an order of magnitude lower than during the other months. The analysis shows that in the tropics, like in the northern mid latitudes, the highest O_3 concentrations in the upper troposphere are observed upon export from the continental (African) boundary layer.

3.3. Stratosphere

Plate 2 depicts the purely stratospheric O_3 concentration fields. As stated in section 2, these fields cannot be interpreted in terms of the sources of stratospheric O_3, because for that the trajectories are not long enough. Because data coverage below 400 hPa is poor, all data are integrated into a single panel for each season. Stratospheric O_3 concentrations show a strong latitudinal gradient, since the tropopause is much lower at higher latitudes than at lower ones and thus the aircraft fly deeper in the stratosphere at higher latitudes. A striking feature, especially in winter and spring, is the wave-like pattern with O_3 maxima over the northernmost parts of North America and eastern Asia, and a minimum over the Atlantic. Both maxima are downstream of regions of strong overall Lagrangian descent of air [*Stohl*, 2001], which are due to the quasi-permanent troughs over the continents caused by PV conservation as airflows over mountain ranges [*Fleagle and Businger*, 1980].

3.4. STE and TSE Flows

The patterns of the STE and TSE concentration fields (not shown) are similar to the purely stratospheric ones, but at concentration levels that are intermediate between the stratosphere and the troposphere. This suggests a strong stratospheric component of the O_3 contained in these air masses, especially in TSE air masses. STE air masses show also patterns seen in purely tropospheric air, which is indicative of the importance of continental O_3 formation for the global O_3 budget, even in the tropopause region.

3.5. Sensitivity Studies

At the example of summertime tropospheric O_3, we made several sensitivity studies (Plate 3). First, we studied the sensitivity of our results to changes in the duration of the back trajectories. Using 10-day trajectories the results are almost the same as with 8-day trajectories (not shown). Two-day trajectories, while also revealing the upper tropospheric maxima over the continents in summer, are too short to yield appropriate data coverage below 700 hPa. Five-day trajectories (Plate 3a) give results similar to the 8-day trajectories but perhaps identify the continental source regions even better than the 8-day ones. Generally, our main results are very robust against changes in the duration of the back trajectories.

Second, it may be argued that the 2 pvu threshold may include some data that are actually stratospheric or at least stratospherically influenced. Therefore, we lowered the PV threshold to 1 pvu. This decreases the number of available tropospheric data by almost a factor of 2 and reduces the coverage of our climatology. However, both the magnitude and the patterns of the tropospheric O_3 concentration fields are almost identical (Plate 3b) to the results obtained with the 2 pvu threshold.

Third, one may question whether PV alone is sufficient to distinguish between stratosphere and tropo-

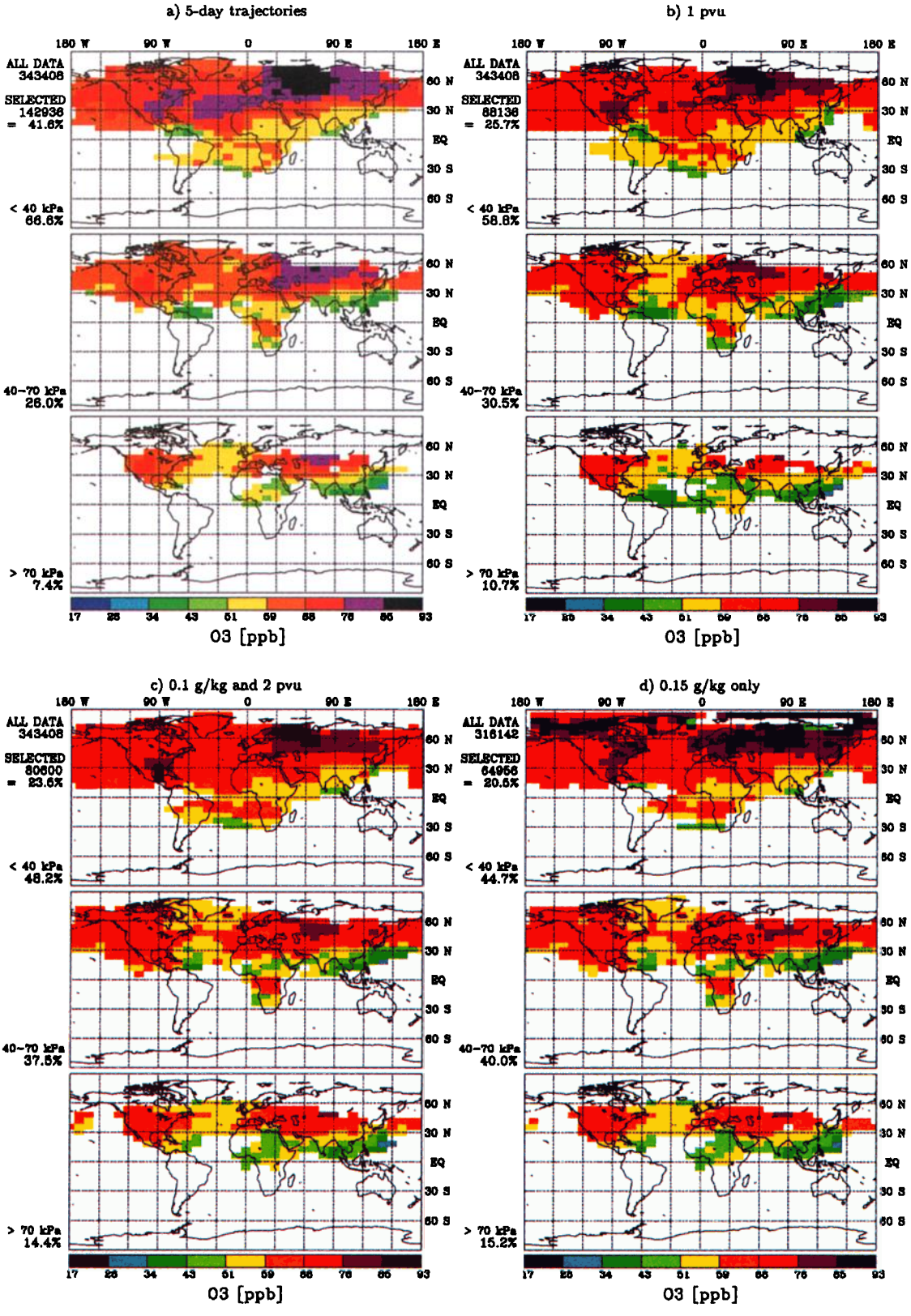

Plate 3. Same as the results for summer shown in Plate 1d, except that different sensitivities are explored: (a) 5-day trajectories were used instead of 8-day trajectories, (b) 1 pvu threshold instead of 2 pvu threshold, (c) 2 pvu threshold and water vapor mixing ratio below 0.1 g^{-1} kg, and (d) water vapor mixing ratio below 0.15 g^{-1} kg. In plate (d) black areas include some O_3 concentrations greater than 93 ppb.

sphere, as fine-scale stratospheric filaments may not be resolved in the ECMWF data. Thus we used, in addition to the 2 pvu threshold, the criterion that the measured water vapor mixing ratio must be greater than 0.1 g^{-1} kg, a value that is typical for the troposphere [*Helten et al.*, 1998]. This reduces the number of available tropospheric data by a factor of 2 but does not change our original results (Plate 3c).

Fourth, Plate 3d shows the effect of using only a humidity threshold. Since it turned out that the threshold of 0.1 g^{-1} kg used previously in conjunction with the 2 pvu threshold still includes many stratospheric data at high latitudes (average O_3 concentrations of several hundred ppb were obtained in some grid cells), we used an even higher value of 0.15 g^{-1} kg. This yields only half of the number of data points obtained with the 2 pvu threshold and is thus a very strict criterion. While the results for the lower two layers are similar to those obtained previously, the results for the uppermost layer still appear to include some stratospherically influenced data points. Thus we conclude that PV is much more efficient than humidity in discriminating between the troposphere and the stratosphere.

4. Conclusions

Trajectory statistics proved to be a powerful tool to analyze the MOZAIC data set in two ways: First, it was possible to extend MOZAIC O_3 climatologies which are otherwise restricted to the major flight corridors. Second, trajectory statistics could shed some light on where tropospheric O_3 is produced, independently from photochemical modeling.

In spring and especially in summer, the North American and Eurasian continental boundary layers are identified as the major sources of O_3 observed in the upper troposphere, while the maritime boundary layers are revealed as O_3 sink regions. In fall and winter the African boundary layer appears to be the greatest O_3 source. At least in summer, STE is clearly less important for upper tropospheric O_3 than photochemical O_3 formation.

The seasonal O_3 variation is much stronger in air masses exported from the continents than in air masses exported from ocean areas. This is valid for both the northern middle latitudes and the tropics. Especially striking is the summer time O_3 maximum in air masses exported from North America and central Asia. The central Asian maximum is higher and occurs earlier (in June) in the year than the North American one (in August). This possibly indicates significant O_3 production from biomass burning emissions in central Asia.

A question that cannot be resolved with our methodology is how much O_3 is produced within the continental boundary layers themselves, and how much is produced on transit from precursors that have been lifted from the continents to the free troposphere. But the relatively short timescales involved point toward export of O_3 itself rather than precursor export followed by O_3 formation.

In the lowermost stratosphere the dominant structure in the O_3 fields is a strong north-south gradient and a wave-like pattern with O_3 maxima over North America and Eastern Asia, likely caused by the stronger descent in these regions than in others.

STE and TSE air masses have O_3 concentrations intermediate between tropospheric and stratospheric values. Both are dominated by stratospheric O_3, but especially STE flows show also some signals of photochemical O_3 formation over the continents.

Acknowledgments. Two reviewers provided exceptionally insightful and constructive comments and suggestions. Thanks are due to P. Fabian for the generous support of our activities. ECMWF and Deutscher Wetterdienst kindly admitted access to ECMWF data. This study was funded by the European Commission as part of the EU projects STACCATO (EVK2-CT-1999-00050), MOZAIC II (ENV4-CT96-0321), and MOZAIC III (EVK2-CT1999-00015), and by the German Federal Ministry for Education and Research in the framework of the Atmospheric Research 2000 program as part of the CARLOTTA project.

References

Ashbaugh, L. L., W. C. Malm, and W. Z. Sadeh, A residence time probability analysis of sulfur concentrations at Grand Canyon National Park, *Atmos. Environ., 19*, 1263-1270, 1985.

Baumann, K., and A. Stohl, Validation of a long-range trajectory model using gas balloon tracks from the Gordon Bennett Cup 95. *J. Appl. Meteorol., 36*, 711-720, 1997.

Beekmann, M., G. Ancellet, and G. Mégie, Climatology of tropospheric ozone in southern Europe and its relation to potential vorticity, *J. Geophys. Res., 99*, 12,841-12,853, 1994.

Benkovitz, c. M., et al., Global gridded inventories of anthropogenic emissions of sulfur and nitrogen, *J. Geophys. Res., 101*, 29,239-29,253, 1996.

Brunner, D., J. Staehelin, and D. Jeker, Large-scale nitrogen oxide plumes in the tropopause region and implications for ozone, *Science, 282*, 1305-1309, 1998.

Cahoon, D. R. Jr., B. J. Stocks, J. S. Levine, W. R. Cofer III, and K. P. O'Neill, Seasonal distribution of African savanna fires, *Nature, 359*, 812-815, 1992.

Christian, C., et al., Global frequency and distribution of lightning as observed by the optical transient detector (OTD), paper presented at 11th International Conference on Atmospheric Electricity, Guntersville, Ala., June 7-11, 1999.

Crawford, J., et al., An assessment of ozone photochemistry in the extratropical western North Pacific: Impact of continental outflow during the late winter/early spring, *J. Geophys. Res., 102*, 28,469-28,487, 1997.

European Centre for Medium-Range Weather Forecasts (ECMWF), User Guide to ECMWF Products 2.1, *Meteorol. Bull. M3.2*, Reading, England, UK, 1995.

Fishman, J., C. E. Watson, J. C. Larsen, and J. A. Logan, Distribution of tropospheric ozone determined from satellite data, *J. Geophys. Res., 95*, 3599-3617, 1990.

Fleagle, R. G., and J. A. Businger, *An Introduction to Atmospheric Physics*, 2nd ed., Academic, San Diego, Calif., 1980.

Helten, M., et al., Calibration and performance of automatic compact instrumentation for the measurement of relative humidity from passenger aircraft, *J. Geophys. Res., 103*, 25,643-25,652, 1998.

Jacob, D. J., et al., Origin of ozone and NO_x in the tropical

troposphere: A photochemical analysis of aircraft observations over the South Atlantic basin, *J. Geophys. Res., 101*, 24,235-24,250, 1996.

Law, K., et al., Comparison between global chemistry transport model results and measurement of ozone and water vapor by airbus in-service aircraft (MOZAIC) data, *J. Geophys. Res., 105*, 1503-1525, 2000.

Lelieveld, J., and F. J. Dentener, What controls tropospheric ozone?, *J. Geophys. Res., 105*, 3531-3551, 2000.

Liu, S. C., M. Trainer, F. C. Fehsenfeld, D. D. Parrish, E. J. Williams, D. W. Fahey, G. Hubler, and P. C. Murphy, Ozone production in the rural troposphere and the implications for regional and global ozone distributions, *J. Geophys. Res., 92*, 4191-4207, 1987.

Logan, J. A., An analysis of ozonesonde data for the troposphere: Recommendations for testing 3-D models and development of a gridded climatology for tropospheric ozone, *J. Geophys. Res., 104*, 16,115-16,150, 1999.

Marenco, A., et al., Measurement of ozone and water vapor by Airbus in-service aircraft: The MOZAIC airborne program, An overview. *J. Geophys. Res., 103*, 25,631-25,642, 1998.

Miller, J. M., The use of back air trajectories in interpreting atmospheric chemistry data: A review and bibliography, *NOAA Tech. Memo., ERL ARL-155*, 60 p., 1987.

Moody, J. L., and J. N. Galloway, Quantifying the relationship between atmospheric transport and the chemical composition of precipitation on Bermuda, *Tellus, 40B*, 463-479, 1988.

Newell, R. E., et al., Ubiquity of quasi-horizontal layers in the troposphere, *Nature, 398*, 316-319, 1999.

Oltmans, S. J., and H. Levy II, Surface ozone measurements from a global network, *Atmos. Environ., 28*, 9-24, 1994.

Parrish, D. D., J. S. Holloway, M. Trainer, P. C. Murphy, G. L. Forbes, and F. C. Fehsenfeld, Export of North American ozone pollution to the North Atlantic Ocean, *Science, 259*, 1436-1439, 1993.

Parrish, D. D., M. Trainer, J. S. Holloway, J. E. Yee, M. S. Warshawsky, F. C. Fehsenfeld, G. L. Forbes, and J. L. Moody, Relationships between ozone and carbon monoxide at surface sites in the North Atlantic region, *J. Geophys. Res., 103*, 13,357-13,376, 1998.

Parrish, D. D., et al., Mixing of anthropogenic pollution with stratospheric ozone: A case study from the North Atlantic wintertime troposphere, *J. Geophys. Res., 105*, 24,363-24,374, 2000.

Prados, A. I., et al., Transport of ozone and pollutants from North America to the North Atlantic Ocean during the 1996 AEROCE intensive experiment, *J. Geophys. Res., 104*, 26,219-26,234, 1999.

Seibert, P., et al., Trajectory analysis of aerosol measurements at high alpine sites, in *Transport and Transformation of Pollutants in the Troposphere*, edited by P. M. Borrell, P. Borrell, T. Cvitaš, and W. Seiler, pp. 689-693, Academic, San Diego, Calif., 1994.

Stohl, A., Trajectory statistics - a new method to establish source-receptor relationships of air pollutants and its application to the transport of particulate sulfate in Europe. *Atmos. Environ., 30*, 579-587, 1996.

Stohl, A., Computation, accuracy and applications of trajectories: A review and bibliography, *Atmos. Environ., 32*, 947-966, 1998.

Stohl, A., A 1-year Lagrangian "climatology" of airstreams in the northern hemisphere troposphere and lowermost stratosphere, *J. Geophys. Res., 106*, 7263-7279, 2001.

Stohl, A., and P. Seibert, Accuracy of trajectories as determined from the conservation of meteorological tracers, *Q. J. R. Meteorol. Soc., 124*, 1465-1484, 1998.

Stohl, A., and T. Trickl, A textbook example of long-range transport: Simultaneous observation of ozone maxima of stratospheric and North American origin in the free troposphere over Europe, *J. Geophys. Res., 104*, 30,445-30,462, 1999.

Stohl, A., G. Wotawa, P. Seibert, and H. Kromp-Kolb, Interpolation errors in wind fields as a function of spatial and temporal resolution and their impact on different types of kinematic trajectories, *J. Appl. Meteorol., 34*, 2149-2165, 1995.

Stohl, A., N. Spichtinger-Rakowsky, P. Bonasoni, H. Feldmann, M. Memmesheimer, H. E. Scheel, T. Trickl, S. Hübener, W. Ringer, and M. Mandl, The influence of stratospheric intrusions on alpine ozone concentrations, *Atmos. Environ., 34*, 1323-1354, 2000.

Thompson, A., et al., Tropical tropospheric ozone and biomass burning, *Science, 291*, 2128-2132, 2001.

Thouret, V., A. Marenco, P. Nédélec, and C. Grouhel, Ozone climatologies at 9-12 km altitude as seen by the MOZAIC airborne program between September 1994 and August 1996, *J. Geophys. Res., 103*, 25,653-25,679, 1998.

Vaughan, G., and C. Timmis, Transport of near-tropopause air into the lower midlatitude stratosphere, *Q. J. R. Meteorol. Soc., 124*, 1559-1578, 1998.

Vaughan, G., J. D. Price, and A. Howells, Transport into the troposphere in a tropopause fold, *Q. J. R. Meteorol. Soc., 120*, 1085-1103, 1994.

Wotawa, G., and H. Kröger, Testing the ability of trajectory statistics to reproduce emission inventories of air pollutants in cases of negligible measurement and transport errors, *Atmos. Environ., 33*, 3037-3043, 1999.

Wotawa, G., and M. Trainer, The influence of Canadian forest fires on pollutant concentrations in the United States. *Science, 288*, 324–328, 2000.

C. Forster, P. James, A. Stohl, and N. Spichtinger, Lehrstuhl für Bioklimatologie und Immissionsforschung, Technische Universität München, Am Hochanger 13, D-85354 Freising-Weihenstephan, Germany. (as@atmos1.met.forst.uni-muenchen.de)

A. Marenco, and V. Thouret, Laboratoire d'Aérologie, UMR 5560, Centre National de Recherche Scientifique / Université Paul Sabatier, 14 Avenue Edouard Belin, 31400 Toulouse, France. (mara@aero.obs-mip.fr)

H. G. J. Smit, Forschungszentrum Jülich, Institut für Chemie der Belasteten Atmosphäre, 52425 Jülich, Germany. (H.Smit@fz-juelich.de)

(Received April 19, 2001; revised July 6, 2001;
accepted July 7, 2001.)